processes

MDPI

Article

A Study on the Thermal Behavior of Series and Parallel Connection Methods in the Process of Hydrogenation of Ship-Borne Hydrogen Storage Cylinder

Jiqiang Li [1,*,†], Jiabao Wang [1,†], Tong Wu [1], Jichao Li [2,*] and Jeong-Tae Kwon [3,*]

[1] School of Transportation, Ludong University, Yantai 264025, China; wjb371328@outlook.com (J.W.); wutong3224599684@163.com (T.W.)
[2] School of Industry, Jining University, Qufu 273155, China
[3] Division of Mechanical & Automotive Engineering, Hoseo University, Asan 31499, Republic of Korea
* Correspondence: ljq7436@ldu.edu.cn (J.L.); jichaojnxy@163.com (J.L.); jtkwon@hoseo.edu (J.-T.K.)
† These authors contributed equally as first authors.

Abstract: As a subdivision of the hydrogen energy application field, ship-borne hydrogen fuel cell systems have certain differences from vehicle or other application scenarios in terms of their structural type, safety, environmental adaptability, and test verification. The connection method of the ship-borne hydrogen storage cylinder (SHSC) is very important for the hydrogen fuel cell ship, and the structural parameters of the SHSC are particularly important in the hydrogen refueling process. To ensure the safe and reliable operation of the hydrogen-powered ship, research on the filling of the SHSC under different connection modes was carried out during refueling. In our study, a thermal flow physical model of the SHSC was established to research the hydrogen refueling process of the series and parallel SHSCs. The influence of series and parallel modes of the SHSCs on the hydrogen refueling process was explored, and the evolution law of the internal flow field, pressure, and temperature of series and parallel SHSCs under different filling parameters was analyzed by numerical simulation. Our results confirmed the superiority of the parallel modular approach in terms of thermal safety during refueling. The results can supply a technical basis for the future development of hydrogen refueling stations and ship-board hydrogenation control algorithms.

Keywords: ship-borne hydrogen storage cylinder; thermal effect; series connection; parallel connection; hydrogen refueling; hydrogen safety

Citation: Li, J.; Wang, J.; Wu, T.; Li, J.; Kwon, J.-T. A Study on the Thermal Behavior of Series and Parallel Connection Methods in the Process of Hydrogenation of Ship-Borne Hydrogen Storage Cylinder. *Processes* **2024**, *12*, 366. https://doi.org/10.3390/pr12020366

Academic Editor: Kian Jon Chua

Received: 4 January 2024
Revised: 29 January 2024
Accepted: 4 February 2024
Published: 10 February 2024

1. Introduction

In the primitive period, the energy used by people came from the sun, which produces light and heat through radiation. Nowadays, many energy sources, including coal, oil, and natural gas, are also indirectly or directly converted by the sun's energy. In 1854, with the first oil well in the world, the world entered the "oil age". Human beings have invented internal combustion engines fueled by gasoline and diesel, and petroleum resources are widely used in automobiles, aviation, navigation, and heavy machinery [1]. With the development of society and the improvement of the economy, human beings have an increasing demand for petroleum, but it is difficult for petroleum products to degrade naturally after being abandoned, polluting land resources; additionally, petroleum combustion reacts with oxygen in the air to produce carbon dioxide. A large amount of carbon dioxide accumulation causes the greenhouse effect and therefore causes global warming. Cargo exchanged between countries is mainly transported by sea. Data released by the International Maritime Organization (IMO) show that the annual carbon emissions of the shipping industry are approximately 1.076 billion tons, accounting for 2.89% of the world's total carbon dioxide emissions and contributing to increasing global warming [2].

Therefore, there is an urgent need for clean energy to replace the current energy used in shipping.

As a result, hydrogen energy, ammonia, methanol, and other clean energy forms have been developed. Methanol is considered a possible alternative to conventional fuels for use in engines [3]. The International Energy Agency (IEA) report that ammonia is the primary low-emission fuel used to decarbonize shipping, with the contributions from biofuels and hydrogen limited in large part by their relatively high costs. Large prototypes of ammonia-fueled ships are being built, methanol-powered container ships are being delivered, and small-scale hydrogen fuel cell ferries are starting operations [4]. Methanol has a high octane number and good explosion resistance, which can appropriately increase the engine compression ratio and improve the combustion efficiency of mixed fuel [5]. Methanol is liquid at room temperature and pressure and can be made from any carbon-containing material by thermochemical methods. The preparation cost is low, the existing fuel storage and transportation equipment can meet the basic requirements, and the transformation cost is low [6,7]. However, the latent heat of vaporization is high, so it is difficult to start at low temperatures when it is used in compression ignition engines [8]. Volumetric H_2 density is the most important factor to consider in transportation. Ammonia has a higher volumetric hydrogen density, which means that more hydrogen can be transported in ammonia in a carrier of the same size. Ammonia has the advantage of requiring relatively little energy to liquefy and is relatively easy to handle. However, ammonia requires energy to crack, and additional energy is needed to increase ammonia's purity [9]. However, the low combustion rate and high spontaneous combustion temperature of ammonia lead to a poor combustion effect of pure ammonia. Additionally, ammonia easily produces harmful NOx under lean combustion conditions [10–12].

Hydrogen, as a major carrier of energy, has the characteristics of a high caloric value, a high energy conversion rate, zero emissions, low vibration and noise, etc. In the case of increasingly stringent requirements for ship emission pollution control, hydrogen energy is gradually becoming a direction of new energy development [13]. Renewable hydrogen plays a critical role in the current energy transition and can facilitate the decarbonization and defossilization of hard-to-abate sectors, such as the industrial, power, transportation, and building sectors. Governments worldwide are implementing ambitious policies to support the establishment of hydrogen technologies, while numerous projects and investments are dedicated to this field. This momentum is accelerating cost and efficiency improvements across the complete renewable hydrogen value chain. However, significant research and advancements in hydrogen production, storage, and utilization infrastructure are still necessary for the widespread adoption of hydrogen technologies. Hydrogen energy is a key technology in addressing fuel pollutants and greenhouse gas emissions, and hydrogen storage tanks are key facilities in insuring hydrogen fuel storage and transportation.

Hydrogen energy is an important method for facilitating carbon reduction in the transport sector. Hydrogen storage tanks (HSTs) are the primary infrastructure for the plant-scale development of hydrogen energy and the core of the fuel cell hyperbaric hydrogen storage system. The efficiency and safety of their charging process have always attracted attention [14]. Li et al. [15] conducted an experimental study on the aging of a thermoplastic gasket of a Type IV composite HST in order to ensure the safety performance of the HST. Zhao et al. [16] carried out a cold compression method for hydrogen storage and performed theoretical and simulation research on the winding of multi-layer carbon fiber in HSTs. Oh et al. [17] simulated the thermal characteristics of the HST, verified the exactitude of the simulation with empirical data, and confirmed the relationship between the Reynolds number and Nusselt number. Hu et al. [18] established a carbon fiber composite HST model to study its failure behaviors. Park et al. [19] established a hydrogen temperature prediction model at the outlet of the pipeline to imitate the transient temperature change in hydrogen from the pre-cooler to the on-board HST during refueling. Zhao et al. [20] built a 2D model of a Type III HST to investigate the temperature distribution and evolution of hydrogen during refueling. Wei et al. [21] established a liquid HST model and investigated the

refueling hydrogen under different shaking conditions. Sapre et al. [22] studied the effect of refueling parameters on the storage density of the tank and analyzed the parameters of the hydrogen refueling station and the on-board HST to improve the storage density of the tank. Taichi et al. [23] built a thermodynamic model for hydrogen refueling stations to simulate the real refueling procedure of supplying hydrogen from high pressure tanks at hydrogen refueling stations to on-board HSTs. Sapre et al. [24] studied the mechanical and thermal reaction of HSTs under different fueling conditions, and the results suggested that the simulated data of tank explosion pressure were in good consistency with the experimental data. Li et al. [25] set up a 3D model of an HST, studied its heat transfer characteristics, and explored the influence of the mass flow rate and heat transfer coefficient on temperature rise during refueling. Zheng et al. [26] established a thermodynamic model to study the thermal insulation scheme of a liquid HST, and the simulation results matched the experimental data well. Li et al. [27] established a new refueling approach based on deep reinforcement learning and proposed a new variable mass flow filling strategy. Xiao et al. [28] established a physical model of an HST to simulate the temperature of hydrogen during refueling. However, this model ignored the heat transfer between the lining and the winding layer, which made the final temperature acquired by the simulation higher than the experimental data. Qiu et al. [29] studied the effect of pressure and power on the mass flow rate and heat transfer characteristics. Wu et al. [30,31] simulated the layered filling process under different conditions which could reach the maximum temperature limit, but the layered filling increased the refueling time. Li et al. [32] determined several effective filling control strategies by studying the temperature rise changes in hydrogen, but they did not conduct a thorough analysis of the top-fit filling strategy. Rothuizen and Rokni [33] studied the effect of the number of stages involved in filling a high-pressure HST on the energy consumption of hydrogen fueling stations, and the results expressed that the energy consumption decreased as the number of stages increased. At present, most hydrogen refueling stations use three-stage high-pressure HSTs. Xiao et al. [34] investigated the pressure configuration of the three-stage HST, and the results showed that the total energy consumption grew approximately linearly with the increase in the hydrogen pressure, while showing a concave curve with the increase in the low and medium pressure stages. Ramasamy et al. [35] researched the hydrogen refueling procedure of HSCs with different length–diameter ratios. Vladimir et al. [36] provided a new method based on entrainment theory to calculate the internal gas temperature change in the HSC during refueling and verified the effectiveness of this method through filling experiments. Deymi-Dashtebayaz et al. [37] studied the hydrogen filling process based on the thermodynamic analysis method. Zhao et al. [38] analyzed the thermal effect of the high-pressure tank pressure relief process through the established thermodynamic model and contrasted the experimental results with the analytical results, verifying the effectiveness of the established model. Bai et al. [39] simulated the rapid compression and filling of hydrogen through the mathematical model of the hydrogen station storage system established and proposed an optimized filling algorithm. The use of other turbulence models for hydrogen fueling simulations is reviewed and summarized by Bourgeois et al. [40], such as Spalart and Allmaras [41], standard k-ε [42], high Reynolds number k-ε [43], realizable k-ε [44], RNG k-ε [45,46], and Reynolds stress (RSM) models [47].

Although many studies have established physical models of the refueling process, these have some shortcomings. Some models used an oversimplified hydrogen equation of state, which led to a certain deviation under high pressure [48]. Some models only considered compressor energy consumption and precooling energy consumption before hydrogenation and did not consider the cooling energy consumption of the compression process. Some models only considered a single hydrogenation and did not consider the change in energy consumption after multiple hydrogenations. In the case of complex flow regimes like transitional flows and stratified temperature fields, the more advanced the turbulence models (e.g., scale-adaptive simulation (SAS) [49] or even LES when possible) used, the more accurate the results obtained. The fatigue damage law of hydrogen cylinders can

be mastered by the experimental study of filling and discharging at different temperatures. However, considering certain risks in charging and discharging experiments, the numerical calculation approach can also be used to predict the temperature changes in the cylinder on the basis of the experiment to provide a basis for its safety evaluation. However, there are still few relevant studies. The marine hydrogen storage system mainly uses a Type III hydrogen storage cylinder lined with aluminum alloy; its hydrogenation temperature rise characteristics have been studied, but the safety boundary conditions for hydrogenation are lacking [50]. Due to the differences in the design of the cylinder structure, even if the same type of hydrogen storage cylinder was used, the thickness and physical characteristics of the lining or winding layer material also led to different hydrogenation temperature rise characteristics. With the rapid growth of the hydrogen energy industry in China, the differences in the structural designs and materials of fuel cell marine hydrogen storage system poses new challenges for the temperature rise management and safety guarantees in hydrogenation operation.

In brief, previous research has focused on the influence of hydrogen cylinder linings and fiber materials on the temperature rise in cylinders. Nevertheless, studies on the structural optimization of HSTs have been limited. In view of the problems of large internal temperature fluctuation and the long adjustment times of the hydrogen tank during the operation of the current hydrogen fuel ship system, it is indispensable to study the thermal effects of the SHSC. The SHSC will produce a significant temperature effect during the fast filling process, which has a significant influence on the strength, fatigue, and effective hydrogen supply of the compound material hydrogen cylinder. In this study, the determining factors and influencing factors of the charging temperature effect were obtained through the analysis of the simplified theoretical model. It is of great necessity to research the influence of SHSC filling processes on the temperature rise in hydrogenation and guide the establishment of a safe hydrogenation method based on the hydrogenation process in HSTs.

2. Hydrogen Refueling Process Modeling

2.1. Hydrogen Refueling Protocol 4

The hydrogen refueling process must be regulated through standardized hydrogen refueling protocols. Currently, the automotive industry uses the American Society of Automotive Engineers SAEJ2601 hydrogenation protocol [51,52], and the latest version is the 2020 revision. The scope of the SAEJ2601 protocol includes on-board HSTs with a volume of 49.7–248.6 L and pressure classes of 35 MPa and 70 MPa, as well as on-board HSTs larger than 248.6 L and 70 MPa. This paper studies a Marine HST with a pressure of 70 MPa. Since there is no hydrogenation protocol for Marine HSTs, the on-board filling protocol is implemented.

2.2. Computational Fluid Dynamics Simulations

2.2.1. Hardware and Software Tools

When building the model, the hardware adopts workstation and is configured as such: the operating system is Windows 10, the CPU is an AMD Ryzen 9 7945HX with Radeon Graphics 5.40 GHz, the RAM size is 32.0 GB, and the ROM size is 2 TB. The graphics card uses NVIDIA GeForce RTXTM4080 and the software uses Fluent 2019R3.

2.2.2. Model Assumption

Considering the complexity of the refueling, in order to simplify the resolution process of the physical model, the following assumptions are made:

(1) The mechanical performance of the SHSC is stable, and the flow channel in the SHSC does not produce structural deformation with the change in pressure and temperature.
(2) The temperature and pressure parameters of the air source upstream of the SHSC are stable, and there is no change in temperature and pressure in the refueling process.

(3) Heat exchange between the SHSC and the surroundings can take place during the refueling, and the heat transfer coefficient is assumed to be a constant, 10 W/m^2K [32].
(4) During the refueling, there is only pure high-pressure hydrogen in the hydrogen refueling system and no other gas impurities, ignoring the influence of gravity.
(5) The inner surface of the HST is smooth enough that the friction effect with hydrogen is ignored and the temperature change is only caused by the throttling, compression, and conversion of the kinetic energy into thermal energy.

2.2.3. The Governing Equations

In this paper, flow analysis used the Navier–Stokes equations, which are based on three equations: the continuous equation, the momentum equation, and the energy equation. Since the fluid flow inside the hydrogen storage container applied in this analysis is turbulent, the flow analysis mainly simulated and interpreted the turbulent flow. In order to predict the turbulent flow, the Fabre averaged butterfly Stokes equation was used, and the time-averaging effect of the flow turbulence on the flow parameters was taken into account in order to solve simultaneous equations involving the turbulent kinetic energy dissipation rate (k-ε models) for the transport equation.

For the heat and flow analysis of the solenoid valve for hydrogen supply, the continuous equation, the momentum equation, and the energy equation were applied as the governing equations, respectively, as shown in Equations (1)–(3).

Continuity equation:

$$\frac{\partial}{\partial t}(\rho) + \frac{\partial}{\partial x_i}(\rho u_i) = 0, \tag{1}$$

Momentum conservation equation:

$$\frac{\partial}{\partial t}(\rho u_i) + \frac{\partial}{\partial x_j}(\rho u_i u_j) = \frac{\partial p}{\partial x_i} + \frac{\partial \tau_{ij}}{\partial x_j} +]\rho F_i, \tag{2}$$

Energy conservation equation:

$$\frac{\partial}{\partial t}(\rho E) + \frac{\partial}{\partial x_i}(u_i(\rho E + p)) = \frac{\partial}{\partial x_j}\left[\left(k + \frac{c_p \mu_t}{Pr_i}\right)\frac{\partial T}{\partial x_j} + u_i \tau_{ij}\right], \tag{3}$$

$$\frac{\partial}{\partial t}(\rho k) + \frac{\partial}{\partial x_i}(\rho k u_i) = \frac{\partial}{\partial x_j}\left[\left(\mu + \frac{\mu_t}{\sigma_k}\right)\frac{\partial k}{\partial x_j}\right] + G_k + G_b - \rho\varepsilon - Y_M + S_k, \tag{4}$$

$$\frac{\partial}{\partial t}(\rho k) + \frac{\partial}{\partial x_i}(\rho \varepsilon u_i) = \frac{\partial}{\partial x_j}\left[\left(\mu + \frac{\mu_t}{\sigma_\varepsilon}\right)\frac{\partial k}{\partial x_j}\right] + C_1\frac{\varepsilon}{k}(G_k + G_b C_3) - C_2\rho\frac{\varepsilon^2}{k} + S_\varepsilon, \tag{5}$$

The k and ε of the model were used in Equations (4) and (5). The two terms on the left side and the first term on the right side of the two expressions denote the time term, convective term, and diffusion term, respectively, and consist of the total extinction rate change amount (Y_M) and custom source term (S_k) in compressible turbulence. The Eddy viscosity in the k-ε model was defined as $\mu_t = \rho C_\mu k^2/\varepsilon$.

2.2.4. Geometric and Grid Independence Verification

In Figure 1, (a) is a 2D model of a hydrogen storage cylinder in series mode and (c) is a 2D model of a hydrogen storage cylinder in parallel mode, while (b) is a 3D model of the hydrogen storage cylinder in series mode and (d) is a 3D model of the hydrogen storage cylinder in parallel mode. In order to distinguish different hydrogen storage cylinders, serial numbers from 1–6 are set for each cylinder in series–parallel mode. The 2D model size of a hydrogen storage cylinder in series and parallel mode are shown in Table 1.

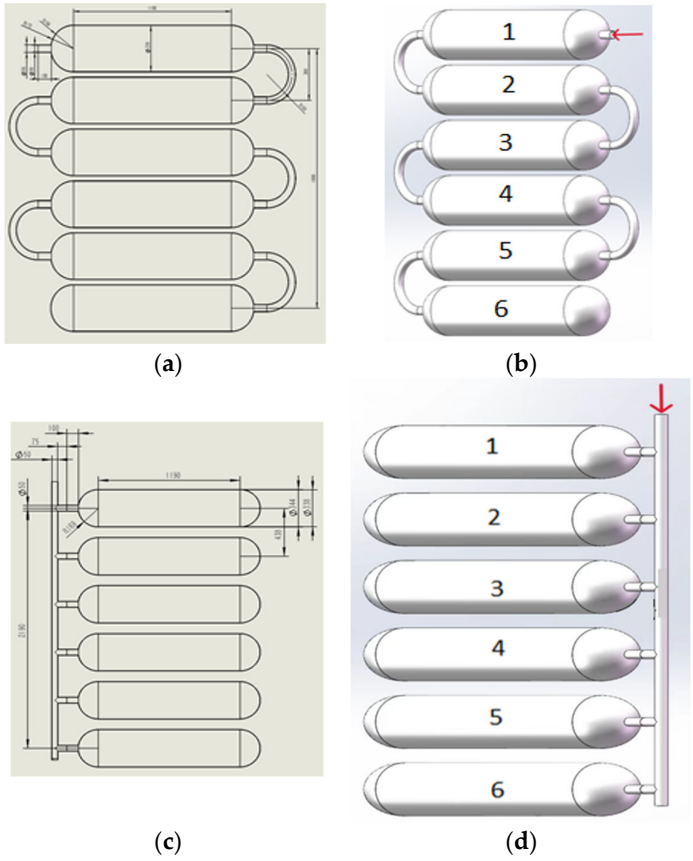

Figure 1. The model for the SHSCs: (**a**) Series: 2D specification; (**b**) Series: 3D; (**c**) Parallel: 2D specification; (**d**) Parallel: 3D.

Table 1. 2D model size of a hydrogen storage cylinder in series and parallel mode.

Item	Size (mm)	
	Series	**Parallel**
Diameter of hydrogen storage tank	338	338
Length of hydrogen storage tank	1528	1528
Distance between center lines of hydrogen storage tanks 1 and 6	1900	2190
Hydrogen storage tanks mouth diameter	50	50
Distance between of two adjacent hydrogen storage tanks	380	438
Internal diameter of pipe	50	50
Length of connecting horizontal tubes	100	175

The temperature of hydrogen in the first 30 s of refueling was regarded as the criterion for the grid independence verification, as listed in Table 1. The temperature rise difference based on the number of 452,874 grids is large, the number of grids increased constantly when the number of grids increased to 981,456, and the average temperature inside the cylinder effectively did not change with time. Therefore, the number of grids is 981,456 for the numerical simulation calculation.

The grid independence of the numerical model was tested. Table 2 shows the temperature and maximum error for different mesh numbers.

Table 2. Mesh size for the grid dependency test.

Mesh Number	Temperature (K)	Max. Error (%)
158,326	339.7	0.65
452,874	336.2	0.50
981,456	332.3	0.30
1,512,345	331.1	0.25

2.2.5. Turbulence Model

The standard k-ε turbulence model, which is widely used to calculate the compressible fluid of valves, was adopted. For the standard k-ε turbulence model, it is necessary to set the Prandtl number to describe the ratio of heat exchange and momentum exchange in the fluid flow process. For the standard k-ε turbulence model, the Prandtl number of the turbulent kinetic energy term was 1.3, the Prandtl number of the turbulent diffusion term was 1 (these two terms were empirical values obtained by experiments based on semi-empirical equations), and the energy Prandtl number and wall Prandtl number were both 0.68 (these two terms were calculated according to the NIST database and the calculation formula for Prandtl numbers).

Table 3 shows the flow rates and miscalculations by different turbulence models. It can be seen that the flow rates calculated by different turbulence models differ little, and, compared with the RNG k-ε turbulence model and realizable k-ε turbulence model, the standard k-ε turbulence model has better convergence. Therefore, the k-ε turbulence model was adopted.

Table 3. Comparison of the calculation results of three turbulence models.

Turbulence Model	Temperature (K)	Max. Error (%)
Standard k-ε	337.9	0.35
RNG k-ε	338.3	0.58
Realizable k-ε	338.5	0.65

2.2.6. Boundary and Initial Condition

Hydrogen is mainly decompressed at the gap, so the geometric parameters in this area will have a great impact on the decompression performance of the pressure reducing valve. Transient numerical simulation of the flow field was carried out. The pressure inlet and outlet boundary conditions were adopted for the inlet and outlet, respectively, and the inlet temperature was set at 293 K. The wall adopted no slip boundary conditions. In order to improve the calculation accuracy, the second-order upwind scheme was adopted for the spatial discretization of pressure, density, momentum, and energy, and the first-order upwind scheme was adopted for the turbulent kinetic energy and turbulent dissipation rate. The time step was 0.001 s.

2.2.7. SHSC Model Validation

The results of numerical simulation of the rapid charging process of the SHSC model need to be verified accurately; therefore, a few sets of experimental data were chosen for validation from references [53,54]. The comparison between the numerical analysis and the experiment is shown in Figure 2. The results indicated that the final temperature of the numerical simulation was slightly different from the experimental value, but the trend was consistent. The temperature error between the numerical simulation results and the data in the references was 2.6%. The numerical simulation results of this paper were correct to a certain extent. The reason for the error may be related to the above assumptions, the error of the model operation, and the limitation of the experimental conditions.

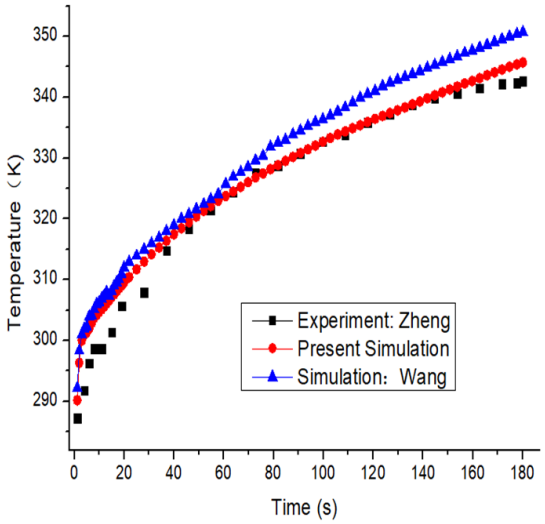

Figure 2. Comparison of the hydrogen temperatures in the experiments and simulations.

3. Results and Discussion

In the actual process of the refueling of the SHSC, the temperature distribution inside the cylinder is affected under different working conditions. Therefore, the refueling process of the SHSC is analyzed, and the objective law of the rapid filling temperature rise in the SHSC is analyzed based on the calculation results.

In order that the numerical simulation results correspond well to the actual background, this paper will study the effects of inflow temperature, initial pressure, and initial temperature on the temperature rise in the SHSC during the refueling by focusing on the series and parallel connection of the SHSCs.

3.1. Thermal Behavior of the SHSC

The inlet temperature of the SHSC during the charging process was set at 263.15 K, the initial pressure in the tank was set at 5 MPa, and the initial temperature of the SHSC was 283.15 K. Hydrogen was charged in a linear pressurization mode, and the settled pressure was 70 MPa.

Figure 3 shows the temperature cloud map inside the SHSC when the charging time, t = 5 s, 10 s, 20 s, 30 s, 50 s, 70 s, and 90 s in parallel state. When hydrogen only filled the SHSC, there was a cyclotron flow at the entrance. With the progress of charging, the cyclotron area gradually expanded until it spread to the entire gas domain. The subsequent charging process tended to be stable, and the duration of this process was relatively short. Because the inlet temperature was low, the inlet hydrogen flow had an obvious temperature gradient, and the hydrogen flow extended along the axis to the middle of the tank. With the progress of charging, the pressure increased gradually, the inlet velocity of hydrogen decreased gradually, and the temperature distribution in the combined hydrogen storage tank was uniform.

Figure 4 displays the velocity distribution in the SHSC with filling times of 0.5 s, 1 s, 5 s, 10 s, 20 s, and 50 s in parallel mode. At the initial time of 0.5 s, relatively obvious hydrogen velocity first appeared in the gas inlet area at the top of the SHSC, while the velocity of hydrogen in the rest of the interior was not obvious and tended to zero. With the passage of time to about 5 s, the speed at the entrance was the highest, and there was a large hydrogen speed at the axis and wall area of the SHSC. After 20 s of fast charging, the velocity distribution inside the cylinder tended to be stable, the hydrogen velocity was the highest at the inlet of the cylinder, and the gas velocity distribution in the SHSC was relatively uniform. It can be seen that the speed of inlet hydrogen was the maximum at different times. With the passage of fast charging time, the speed of inlet hydrogen began to decline, the speed of internal hydrogen also gradually decreased, and the rate of decrease in

hydrogen speed slowly decreased. This is because when the SHSC was quickly charged, the pressure inside the cylinder was increasing, preventing hydrogen from entering the SHSC.

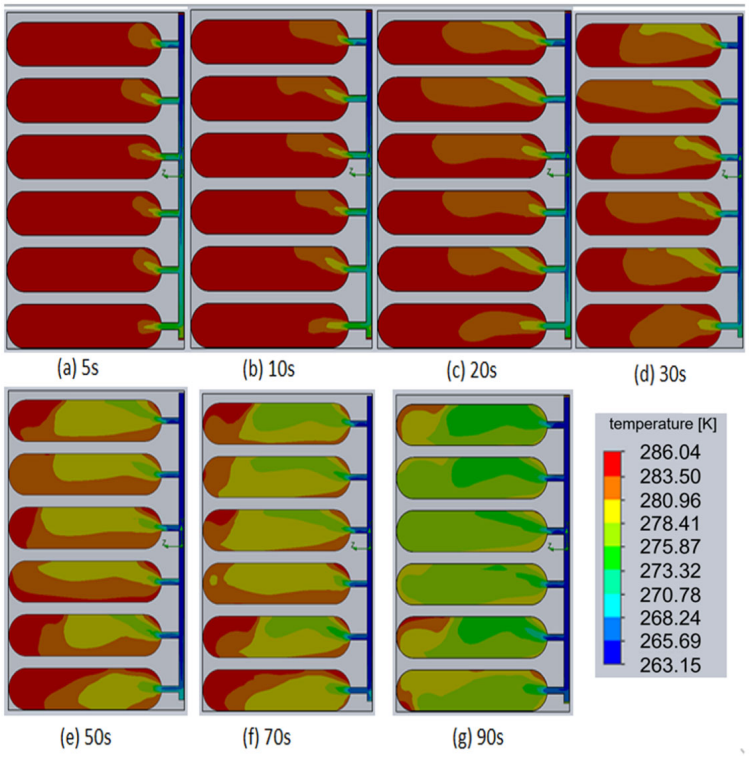

Figure 3. The hydrogen temperature after (**a**) 5 s, (**b**) 10 s, (**c**) 20 s, (**d**) 30 s, (**e**) 50 s, (**f**) 70 s, and (**g**) 90 s of hydrogen refueling for a parallel-type connection module.

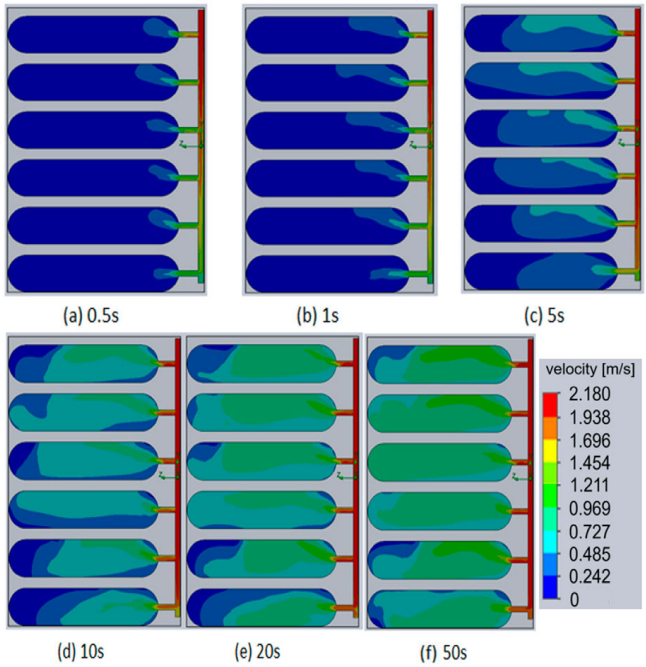

Figure 4. The velocity distributions in hydrogen charging for a parallel-type model at different times.

Figure 5 illustrates the temperature variation over time in the SHSC unloaded in series mode. Due to the low precooling temperature, the overall trend of maximum temperature change over time was not obvious. During the first 5 s period of the fast charging process, the hydrogen in the SHSC decreased first and then increased. After 5 s of fast charging, it

can be observed that the rise rate of the thermal peak constantly changed with the passage of time, and eventually the rise in the maximum temperature tended to be flat. However, before the end of the fast charge, the temperature of the first SHSC under the series mode was the highest. This is because the recirculation flow formed in the SHSC stayed at the top of the inlet of the cylinder along with the incoming jet during the fast charging process, meaning that the heat carried by the hydrogen circulation flow gradually converged at the top area of the cylinder. In the fast-charging mode of the series mode, the high temperature zone easily to appeared, and the temperature distribution of each SHSC was uneven.

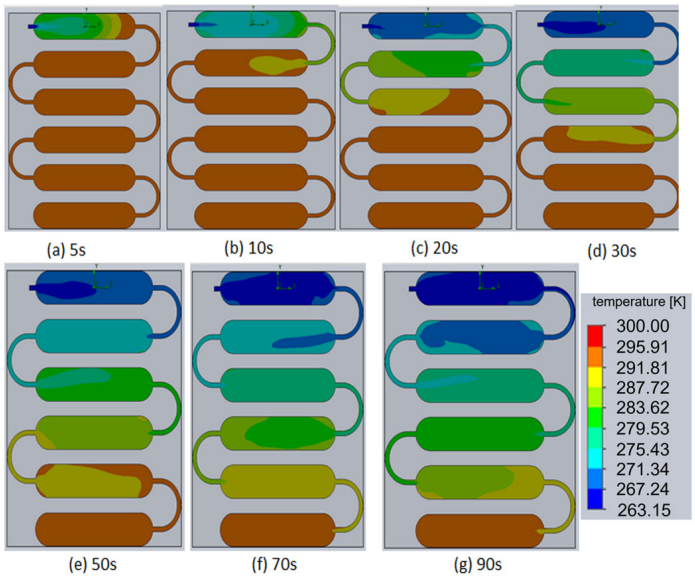

Figure 5. Temperature distributions according to different times for a serial-type SHSC.

The simulation conditions in series mode are the same as those in parallel mode. Figure 6 shows the velocity distribution inside the SHSC in series mode. The results show that there was a relatively obvious hydrogen velocity gradient in the top gas inlet area of the SHSC, and the velocity changed obviously in the inlet area of the SHSC. The inlet speed was the highest, and there was a high hydrogen speed in the axis and wall area of the SHSC while the hydrogen speed was very insignificant in other areas. With the passage of time, the velocity of the first hydrogen storage tank in series mode became larger, and the velocity distribution inside other cylinders was similar as a whole. While the larger velocity region was relatively reduced, the velocity also increased slightly, but this increase was not obvious.

3.2. Effects of Refueling Parameters on the Hydrogen Temperature

3.2.1. Initial Temperature

In order to research the influence of initial temperature on the temperature rise in the SHSC under the series and parallel connection, the volume of the hydrogen storage cylinder was 150 L, the length of the pipeline was 0 mm, the filling began from 5 MPa, and the pressure rose linearly to 70 MPa. The initial temperature and environmental temperature of the fast-charging system are 275 K, 285 K, 295 K, 305 K, and 315 K. In the actual situation, when the hydrogen storage cylinder was rapidly charged, the hydrogen in the hydrogenation system needed to be pre-cooled, so the system imported hydrogen for pre-cooling, and the temperature was 255.15 K. In this paper, it is considered that the ambient temperature in the hydrogen refueling system is the same as the initial temperature of the hydrogen storage tank full of hydrogen.

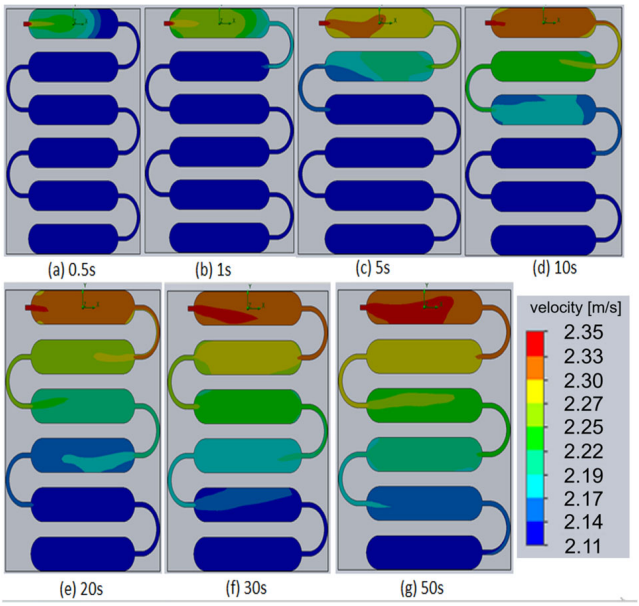

Figure 6. The velocity distributions after (**a**) 0.5 s, (**b**) 1 s, (**c**) 5 s, (**d**) 10 s, (**e**) 20 s, (**f**) 30 s, and (**g**) 50 s of hydrogen refueling for a serial-type SHSC.

Figure 7 shows the variation in the temperature on the inner axis of hydrogen storage cylinders with the distance between the cylinders at different initial temperatures. When hydrogen storage cylinders are in parallel mode, the temperature difference between the hydrogen storage cylinders is relatively small, and the temperature inside the hydrogen storage cylinders increases with the distance from the cylinder mouth. At the distance of 0–0.2 m from the bottle mouth, the temperature is lower than the surrounding temperature because hydrogen is pre-cooled. As shown in Figure 3, the temperature at the bottle mouth is approximately 275 K. When the hydrogen storage cylinder is in series mode, the temperature difference between the hydrogen storage cylinders is relatively large, which is because hydrogen storage cylinder No. 6 is preferentially filled during the hydrogen filling process. As the other cylinders are filled, the temperature of the cylinder at the bottom accumulates and increases, meaning there is a temperature difference between the bottom cylinder and the top cylinder. It can be seen that when the initial pressure of the hydrogen storage flask is 2 MPa and the pressure is quickly charged to 70 MPa, the temperature rise in the hydrogen in the hydrogen storage flask presents a linear increase with the rise in initial temperature, and the growth is relatively slow. The higher the initial temperature, the higher the temperature rise in the hydrogen inside the hydrogen storage flask when the fast charging is completed. When the initial temperature is 275 K, 285 K, or 295 K, the temperature at the completion of filling does not surpass the 358.15 K specified in the code. When the initial temperature is 305 K or 315 K, the temperature at the completion of the filling exceeds the specification of 358.15 K. Obviously, when the initial temperature is 305 K or 315 K, the pre-cooling temperature of hydrogen is 255 K, meaning when the initial temperature exceeds 295 K, the pre-cooling temperature of hydrogen should be less than 255 K. The hydrogen temperature in SHSCs in the parallel mode is 20 K lower than that in the series mode. In the case of high initial temperature, the pre-cooling temperature can be reduced, which can greatly reduce the temperature rise in hydrogen at the conclusion of the fast charge.

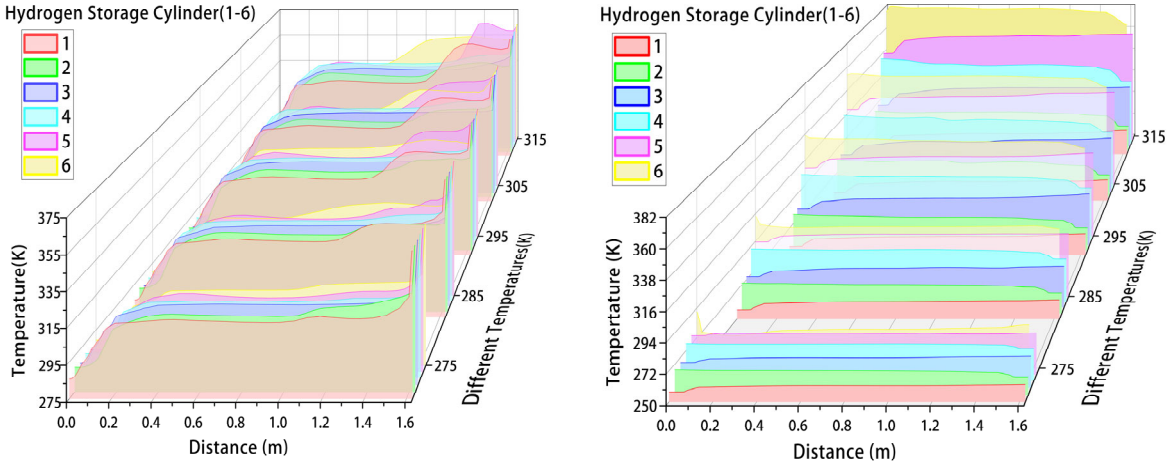

Figure 7. The temperature change in SHSCs under different initial temperatures: (**a**) parallel mode; (**b**) series mode.

3.2.2. Initial Pressure

In an effort to study the influence of initial pressure on the temperature rise in the hydrogen storage cylinder under the series and parallel connection, the simulation conditions were similar to the initial temperature research conditions. The initial pressure of the hydrogen storage cylinder in the fast-charging system was, respectively, 2 MPa, 5 MPa, 10 MPa, 15 MPa, and 20 MPa to start the filling. The linear pressure increased to 70 MPa. In actual conditions, the hydrogen in the hydrogen refueling system needs to be pre-cooled for rapid charging, so the system imports hydrogen for pre-cooling, and the temperature is 255.15 K. In actual conditions, the initial temperature and the ambient temperature are the same for fast charging the hydrogen storage cylinder, so the initial temperature is 283.15 K.

The different initial pressure values in the hydrogen storage cylinder have a certain influence on the temperature, the filling quality, and the filling speed to the target pressure during the hydrogen filling process. When the difference between the initial pressure value in the cylinder and the target pressure value was smaller, the temperature increase during the charging process and the mass of hydrogen injected into the cylinder were smaller, the speed of charging to the target pressure value was accelerated, and the charging time was reduced. In contrast, when the difference between the initial pressure value in the cylinder and the target pressure value was larger, the temperature rise in the charging process and the mass of hydrogen injected into the cylinder were larger, the speed of charging to the target pressure value was slower, and the charging time was longer. Figure 8 shows the maximum temperature variation with time under different initial pressures and the curve of rapid charging temperature with the initial pressure of the hydrogen storage cylinder. It can be noted that when the initial pressure of hydrogen storage cylinder was 2 MPa, 5 MPa, 10 MPa, 15 MPa, and 20 MPa, the pressure quickly charged and increased to 70 MPa. With the rise in initial pressure, the temperature rise in hydrogen in the hydrogen storage cylinder presented a linear downward trend, and the decline speed was rapid. The higher the initial pressure was, the lower the temperature rise in hydrogen in the hydrogen storage cylinder was when the filling was finished. As the initial pressure in the hydrogen storage cylinder increased, the filling completion time became lower and lower. The maximum temperature of hydrogen at the initial pressure of 20 MPa was 21 K lower than that at the initial pressure of 2 MPa.

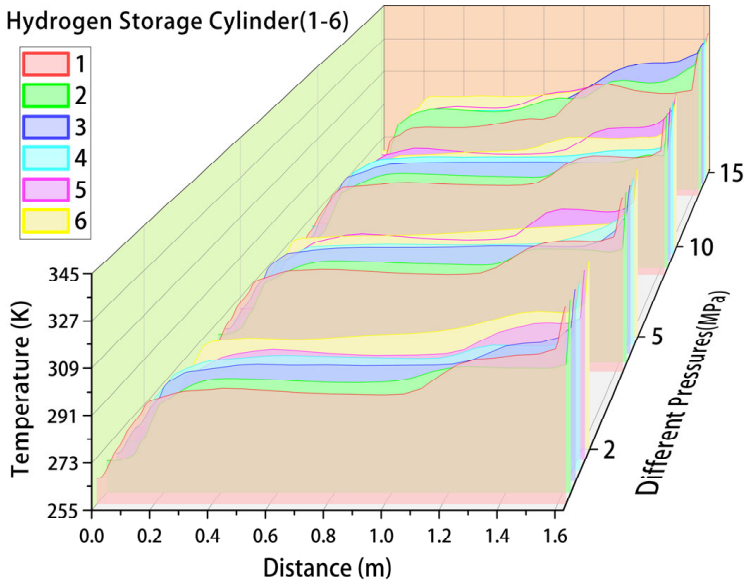

Figure 8. The hydrogen temperature change in the SHSC in the parallel mode.

3.2.3. Pre-Cooled Temperature

In order to study the effect of pre-cooling temperature on the temperature rise in hydrogen storage cylinders under series parallel operation, the simulation conditions were similar to the initial temperature research conditions. The pre-cooling temperatures of the hydrogen storage cylinders in the rapid charging system were 235 K, 245 K, 255 K, 265 K, and 275 K, respectively, and the pre-cooling increased from 5 MPa to 70 MPa. In practice, the initial temperature and ambient temperature of the hydrogen storage cylinder are the same, so the initial temperature was 283.15 K.

Figure 9 indicates the variation in hydrogen temperature with time under different precooling temperatures. Because the filling temperature was lower than the initial temperature in the hydrogen storage cylinder, the temperature in the hydrogen storage cylinder initially dropped; then, with the increase in time, the temperature in the bottle changed from falling to rising. Compared with the series mode, the temperature difference between the hydrogen storage cylinders in the parallel mode was smaller because the charging into the six hydrogen storage cylinders in the parallel mode was more uniform than that in the series mode. The hydrogen charging process in series mode was similar to the accumulation process from the bottom to the top of the hydrogen storage cylinder, so the temperature of hydrogen storage cylinder No. 6 in the series mode was significantly higher than that of other hydrogen storage cylinders; ultimately, the temperature difference, temperature rise, and maximum temperature in series mode were higher than those in parallel mode. When the pre-cooling temperature was 235 K, 245 K, or 255 K, the maximum temperature at the completion of filling did not exceed the specification of 358.15 K. When the inflow temperature was 265 K or 275 K, the temperature in series mode exceeded the 358.15 K specified in the code. The temperature of hydrogen at the pre-cooling temperature of 275 K in series mode was approximately 19 K higher than that at the pre-cooling temperature of 275 K in parallel mode. Under different precooling temperatures, the maximum temperature increased with the rise in the precooling temperature, and the higher the precooling temperature, the more drastic the trend of hydrogen temperature increases. Therefore, parallel connection has more advantages in terms of temperature control.

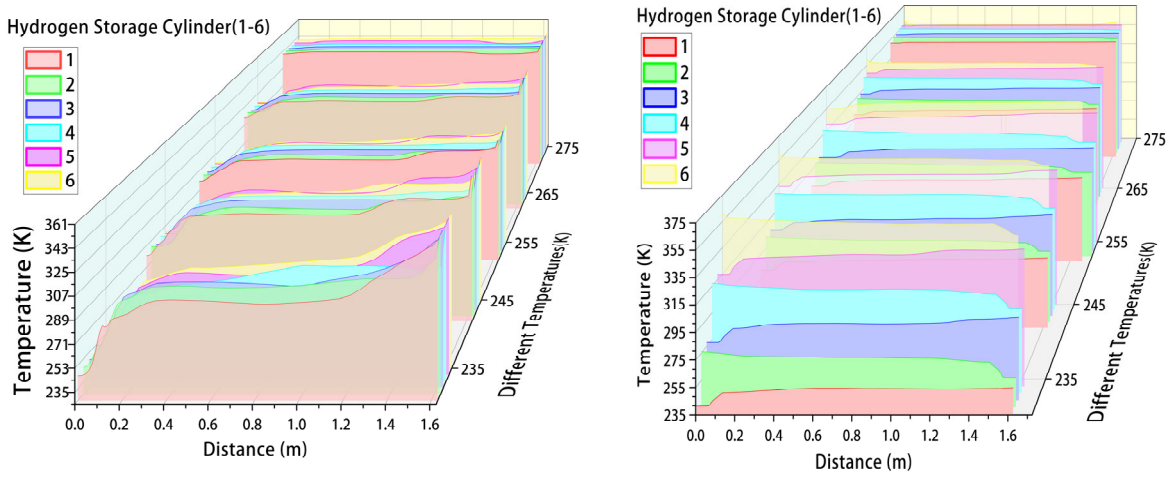

Figure 9. Temperature variations in the SHSCs according to different inflow temperatures. (**a**) parallel mode; (**b**) series mode.

4. Conclusions

As the most promising form of renewable energy, hydrogen energy is used more and more widely, and application of hydrogen energy in ships is of great significance in the development of ships. However, the high-pressure hydrogen provided by the SHSC is very important for hydrogen fuel cell ships. Therefore, the problems encountered in the filling process of the SHSCs are particularly important. In our study, thermal analysis of an SHSC was carried out during refueling. The effect of connection modes on the fast charging of SHSCs was revealed. The effect of refueling parameters on the temperature rise in SHSCs was also analyzed. The major conclusions were as follows:

1. The pressure distribution of the SHSCs under the series method was uneven, and the pressure difference was large during the refueling. The internal pressure difference of series mode was 2.55% higher than that of parallel mode.
2. The temperature distribution of SHSCs in parallel mode was relatively uniform, and the temperature rise was low in the process of refueling. The temperature distribution in SHSCs in series was not uniform, which was easily caused local high temperatures. The temperature rise in parallel mode was 5.85% lower than that in series mode.
3. According to the simulation analysis of the refueling of the series parallel SHSCs under different charging parameters, the superiority of the parallel connection method in terms of thermal safety was verified.
4. The temperature of pre-cooled hydrogen could greatly reduce the temperature rise during the refueling. Controlling the pre-cooling temperature was the most effective and direct strategy to reduce the temperature rise.

The research results provide the following suggestions for the future development of fuel cell hydrogen supply systems: At present, high-pressure gaseous hydrogen storage is the main hydrogen storage method because it is the most practical and effective method. In the process of filling gaseous hydrogen into the hydrogen storage cylinder, it is recommended to pre-cool the hydrogen in the hydrogen storage cylinder to reduce the temperature rise during the hydrogenation process. If there are multiple hydrogen storage cylinders connected to each other, it is recommended to use hydrogen storage cylinders in parallel connection with each other; this can make the pressure rise in the hydrogen storage cylinder relatively uniform while keeping the temperature rise change between the hydrogen storage cylinders relatively small, which has certain advantages for the material protection of the cylinders, can prolong their service life, and improve the safety of the hydrogen filling and the use processes.

Author Contributions: Conceptualization, J.L. (Jiqiang Li), J.L. (Jichao Li) and J.-T.K.; methodology, J.L. (Jiqiang Li), J.L. (Jichao Li) and J.-T.K.; formal analysis J.W. and T.W.; software, J.W.; writing—original draft preparation, T.W. and J.W.; validation, investigation, resources, T.W. and J.W.; data curation, J.L. (Jiqiang Li), T.W. and J.W.; writing—review and editing, J.L. (Jiqiang Li) and J.W.; visualization, J.L. (Jichao Li); supervision, project administration, J.-T.K.; funding acquisition, J.-T.K. All authors have read and agreed to the published version of the manuscript.

Funding: This research was funded by the Regional Innovation Strategy (RIS) through the National Research Foundation of Korea (NRF) funded by the Ministry of Education (MOE) (2021RIS-004).

Data Availability Statement: Data are contained within the article.

Conflicts of Interest: The authors declare no conflict of interest.

References

1. Romero, C.A.; Correa, P.; Ariza Echeverri, E.A.; Vergara, D. Strategies for Reducing Automobile Fuel Consumption. *Appl. Sci.* **2024**, *14*, 910. [CrossRef]
2. Application Status and Prospect Analysis of Hydrogen Energy in Ship Field. Available online: http://www.csoa.cn/doc/24640.jsp (accessed on 9 March 2023).
3. Verhelst, S.; Turner, J.W.; Sileghem, L.; Vancoillie, J. Methanol as a fuel for internal combustion engines. *Prog. Energy Combust. Sci.* **2019**, *70*, 43–88. [CrossRef]
4. Net Zero Roadmap, A Global Pathway to Keep the 1.5 °C Goal in Reach, 2023 Update. International Energy Agency. Available online: https://www.iea.org/events/net-zero-roadmap-a-global-pathway-to-keep-the-1-5-c-goal-in-reach-2023-update (accessed on 26 September 2023).
5. Saxena, M.R.; Maurya, R.K.; Mishra, P. Assessment of performance, combustion and emissions characteristics of methanol-diesel dual-fuel compression ignition engine: A review. *J. Traffic Transp. Eng.* **2021**, *8*, 638–680. [CrossRef]
6. Tian, Z.; Wang, Y.; Zhen, X.; Liu, Z. The effect of methanol production and application in internal combustion engines on emissions in the context of carbon neutrality: A review. *Fuel* **2022**, *320*, 123902. [CrossRef]
7. Shen, Z.; Qu, Q.; Chen, M.; Lyu, H.; Sun, J. Advancements in methanol distillation system: A comprehensive overview. *Chem. Eng. Res. Des.* **2023**, *199*, 130–151. [CrossRef]
8. Huang, Z.; Lyu, Z.; Luo, P.; Zhang, G.; Ying, W.; Chen, A.; Xiao, H. Effects of Methanol–Ammonia Blending Ratio on Performance and Emission Characteristics of a Compression Ignition Engine. *J. Mar. Sci. Eng.* **2023**, *11*, 2388. [CrossRef]
9. Seo, Y.; An, J.; Park, E.; Kim, J.; Cho, M.; Han, S.; Lee, J. Technical–Economic Analysis for Ammonia Ocean Transportation Using an Ammonia-Fueled Carrier. *Sustainability* **2024**, *16*, 827. [CrossRef]
10. Manigandan, S.; Ryu, J.I.; Kumar, T.P.; Elgendi, M. Hydrogen and ammonia as a primary fuel—A critical review of production technologies, diesel engine applications, and challenges. *Fuel* **2023**, *352*, 129100. [CrossRef]
11. Hu, X.; Pan, J.; Zhang, R.; Li, J.; Li, W.; Wei, H. Effects of intake parameters and compression ratio on ammonia combustion and emissions in SI engines. *Fuel* **2023**, *354*, 129382. [CrossRef]
12. Uddeen, K.; Tang, Q.; Shi, H.; Magnotti, G.; Turner, J. A novel multiple spark ignition strategy to achieve pure ammonia combustion in an optical spark-ignition engine. *Fuel* **2023**, *349*, 128741. [CrossRef]
13. Qiu, C.; Chen, S.; Shen, Y.; Tao, X.; Gan, Z. Numerical and experimental study on a tube-in-tube heat exchanger working at liquid-hydrogen temperature with a large temperature span. *Int. J. Heat Mass Transf.* **2023**, *208*, 124089. [CrossRef]
14. Li, J.Q.; Chen, Y.; Ma, Y.B.; Kwon, J.T.; Xu, H.; Li, J.C. A study on the Joule-Thomson effect of during filling hydrogen in high pressure tank. *Case Stud. Therm. Eng.* **2023**, *41*, 102678. [CrossRef]
15. Li, J.; Lv, R.; Gu, C.; Liu, Y.; Li, J.; Li, X. An Ageing Test Standards Analysis on Thermoplastic Liners of Type IV Composite Hydrogen Storage Tanks. *Energies* **2023**, *16*, 2818. [CrossRef]
16. Zhao, X.; Yan, Y.; Zhang, J.; Zhang, F.; Wang, Z.; Ni, Z. Analysis of multilayered carbon fiber winding of cryo-compressed hydrogen storage vessel. *Int. J. Hydrogen Energy* **2022**, *47*, 10934–10946. [CrossRef]
17. Oh, S.J.; Yoon, J.H.; Jeon, K.S.; Choi, J. A study on the thermal characteristics of hydrogen storage vessel related to condition of charging. *J. Mech. Sci. Technol.* **2022**, *36*, 1579–1586. [CrossRef]
18. Hu, Z.; Chen, M.H.; Zu, L.; Jia, X.; Shen, A.; Yang, Q.; Xu, K. Investigation on failure behaviors of 70 MPa Type IV carbon fiber overwound hydrogen storage vessels. *Compos. Struct.* **2021**, *259*, 113387. [CrossRef]
19. Park, B.H.; Lee, D.H. Flow analysis and development of a model to simulate transient temperature of hydrogen from pre-cooler to on-board storage tank during hydrogen refueling. *Korean J. Chem. Eng.* **2022**, *39*, 902–912. [CrossRef]
20. Zhao, B.; Wei, H.; Peng, X.; Feng, J.; Jia, X. Experimental and Numerical Research on Temperature Evolution during the Fast-Filling Process of a Type III Hydrogen Tank. *Energies* **2022**, *15*, 3811. [CrossRef]
21. Wei, G.; Zhang, J. Numerical study of the filling process of a liquid hydrogen storage tank under different sloshing conditions. *Processes* **2020**, *8*, 1020. [CrossRef]
22. Sapre, S.; Vyas, M.; Pareek, K. Impact of refueling parameters on storage density of compressed hydrogen storage Tank. *Int. J. Hydrogen Energy* **2021**, *46*, 16685–16692. [CrossRef]

23. Kuroki, T.; Nagasawa, K.; Peters, M.; Leighton, D.; Kurtz, J.; Sakoda, N.; Monde, M.; Takata, Y. Thermodynamic modeling of hydrogen fueling process from high-pressure storage tank to vehicle tank. *Int. J. Hydrogen Energy* **2021**, *46*, 22004–22017. [CrossRef]
24. Sapre, S.; Pareek, K.; Vyas, M. Investigation of structural stability of type IV compressed hydrogen storage tank during refueling of fuel cell vehicle. *Energy Storage* **2020**, *2*, e150. [CrossRef]
25. Wang, L.; Ye, F.; Xiao, J.; Bénard, P.; Chahine, R. Heat transfer analysis for fast filling of on-board hydrogen tank. *Energy Procedia* **2019**, *158*, 1910–1916. [CrossRef]
26. Zheng, J.; Chen, L.; Wang, J.; Xi, X.; Zhu, H.; Zhou, Y.; Wang, J. Thermodynamic analysis and comparison of four insulation schemes for liquid hydrogen storage tank. *Energy Convers. Manag.* **2019**, *186*, 526–534. [CrossRef]
27. Li, J.; Wang, T.; Yang, Q.; Song, P.; Su, H. Towards fast and safe hydrogen filling for the fuel vehicle: A variable mass flow filling strategy based on a real-time thermodynamic model. *Int. J. Hydrogen Energy* **2023**, *48*, 20406–20418. [CrossRef]
28. Xiao, J.; Wang, X.; Zhou, X.; Bénard, P.; Chahine, R. A dual zone thermodynamic model for refueling hydrogen vehicles. *Int. J. Hydrogen Energy* **2019**, *44*, 8780–8790. [CrossRef]
29. Qiu, Y.; Zhai, H.; Zheng, Y.; Lei, G.; Wang, T.; Wang, L.; Shu, S. Numerical investigation into the natural convection of cryogenic supercritical helium in a spherical enclosure. *Energies* **2021**, *14*, 2584. [CrossRef]
30. Wu, X.; Liu, J.; Deng, G.; Shao, J. Research on Fast Filling Strategy of Large Capacity on-Board Hydrogen Storage Tank for Highway Passenger Cars. SAE Technical Paper, 21–23 April 2020. Available online: https://www.sae.org/publications/technical-papers/content/2020-01-0855/ (accessed on 26 September 2023).
31. Wu, X.; Liu, J.; Shao, J.; Deng, G. Fast filling strategy of type III on-board hydrogen tank based on time-delayed method. *Int. J. Hydrogen Energy* **2021**, *46*, 29288–29296. [CrossRef]
32. Li, M.; Bai, Y.; Zhang, C.; Song, Y.; Jiang, S.; Grouset, D.; Zhang, M. Review on the research of hydrogen storage system fast refueling in fuel cell vehicle. *Int. J. Hydrogen Energy* **2019**, *44*, 10677–10693. [CrossRef]
33. Rothuizen, E.; Rokni, M. Optimization of the overall energy consumption in cascade fueling stations for hydrogen vehicles. *Int. J. Hydrogen Energy* **2014**, *39*, 582–592. [CrossRef]
34. Xiao, L.; Chen, J.; Wu, Y.; Zhang, W.; Ye, J.; Shao, S.; Xie, J. Effects of pressure levels in three-cascade storage system on the overall energy consumption in the hydrogen refueling station. *Int. J. Hydrogen Energy* **2021**, *46*, 31334–31345. [CrossRef]
35. Ramasamy, V.; Richardson, E.S. Thermal response of high-aspect-ratio hydrogen cylinders undergoing fast-filling. *Int. J. Heat Mass Transfer* **2020**, *160*, 120179. [CrossRef]
36. Molkov, V.; Dadashzadeh, M.; Makarov, D. Physical model of onboard hydrogen storage tank thermal behaviour during fuelling. *Int. J. Hydrogen Energy* **2019**, *44*, 4374–4384. [CrossRef]
37. Sadi, M.; Deymi-Dashtebayaz, M. Hydrogen refueling process from the buffer and the cascade storage banks to HV cylinder. *Int. J. Hydrogen Energy* **2019**, *44*, 18496–18504. [CrossRef]
38. Zhao, L.; Li, F.; Li, Z.; Zhang, L.; He, G.; Zhao, Q.; Yuan, J.; Di, J.; Zhou, C. Thermodynamic analysis of the emptying process of compressed hydrogen tanks. *Int. J. Hydrogen Energy* **2019**, *44*, 3993–4005. [CrossRef]
39. Bai, Y.; Zhang, C.; Duan, H.; Jiang, S.; Zhou, Z.; Grouset, D.; Ye, X. Modeling and optimal control of fast filling process of hydrogen to fuel cell vehicle. *J. Energy Storage* **2021**, *35*, 102306. [CrossRef]
40. Bourgeois, T.; Ammouri, F.; Baraldi, D.; Moretto, P. The temperature evolution in compressed gas filling processes: A review. *Int. J. Hydrogen Energy* **2018**, *43*, 2268–2292. [CrossRef]
41. Spalart, P.; Allmaras, S. A one-equation turbulence model for aerodynamic flows. In Proceedings of the 30th Aerospace Sciences Meeting and Exhibit, Reno, NV, USA, 6–9 January 1992; p. 439.
42. Launder, B.; Sharma, B. Application of the energy-dissipation model of turbulence to the calculation of flow near a spinning disc. *Lett. Heat Mass Transf.* **1974**, *1*, 131–137. [CrossRef]
43. Speziale, C.G. On nonlinear kl and k-ε models of turbulence. *J. Fluid Mech.* **1987**, *178*, 459–475. [CrossRef]
44. Shih, T.-H.; Liou, W.W.; Shabbir, A.; Yang, Z.; Zhu, J. A new k-ϵ eddy viscosity model for high reynolds number turbulent flows. *Comput. Fluids* **1995**, *24*, 227–238. [CrossRef]
45. Yakhot, V.; Orszag, S.A. Renormalization group analysis of turbulence. I. Basic theory. *J. Sci. Comput.* **1986**, *1*, 3–51. [CrossRef]
46. Yakhot, V.; Orszag, S.A.; Thangam, S.; Gatski, T.B.; Speziale, C.G. Development of turbulence models for shear flows by a double expansion technique. *Phys. Fluids A Fluid Dyn.* **1992**, *4*, 1510–1520. [CrossRef]
47. Hanjalić, K.; Launder, B.E. A Reynolds stress model of turbulence and its application to thin shear flows. *J. Fluid Mech.* **1972**, *52*, 609–638. [CrossRef]
48. Xie, H.; Makarov, D.; Kashkarov, S.; Molkov, V. CFD Simulations of Hydrogen Tank Fuelling: Sensitivity to Turbulence Model and Grid Resolution. *Hydrogen* **2023**, *4*, 1001–1021. [CrossRef]
49. Menter, F.; Egorov, Y. A scale adaptive simulation model using two-equation models. In Proceedings of the 43rd AIAA Aerospace Sciences Meeting and Exhibit, Reno, NV, USA, 10–13 January 2005; p. 1095.
50. Liu, J.; Ma, H.Q.; Zheng, S.Y.; Zhang, Z.X.; Zheng, J.Y.; Zhao, Y.Z. Numerical Investigation on Temperature-rise of on-bus Gaseous Hydrogen Storage Cylinder with Different Thickness of Liner and Wrapping Material. *Int. J. Hydrogen Energy* **2021**, *46*, 20607–20620. [CrossRef]
51. *J2601_202005*; Fueling Protocols for Light Duty Gaseous Hydrogen Surface Vehicles. SAE International: New York, NY, USA, 2020.

52. Chochlidakis, C.G.; Rothuizen, E.D. Overall efficiency comparison between the fueling methods of SAEJ2601 using dynamic simulations. *Int. J. Hydrogen Energy* **2020**, *45*, 11842–11854. [CrossRef]
53. Zheng, J.; Guo, J.; Yang, J.; Zhao, Y.; Zhao, L.; Pan, X.; Ma, J.; Zhang, L. Experimental and numerical study on temperature rise within a 70 MPa type III cylinder during fast refueling. *Int. J. Hydrogen Energy* **2013**, *38*, 10956–10962. [CrossRef]
54. Wang, L.; Zheng, C.; Wei, S.; Wang, B.; Wei, Z. Thermo-mechanical investigation of composite high-pressure hydrogen storage cylinder during fast filling. *Int. J. Hydrogen Energy* **2015**, *40*, 6853–6859. [CrossRef]